

Toroidal electron temperature gradient driven drift modes

W. Horton, B. G. Hong, and W. M. Tang

Citation: [The Physics of Fluids](#) **31**, 2971 (1988); doi: 10.1063/1.866954

View online: <https://doi.org/10.1063/1.866954>

View Table of Contents: <https://aip.scitation.org/toc/pfl/31/10>

Published by the [American Institute of Physics](#)

ARTICLES YOU MAY BE INTERESTED IN

[Electron temperature gradient driven turbulence](#)

[Physics of Plasmas](#) **7**, 1904 (2000); <https://doi.org/10.1063/1.874014>

[Ion temperature-gradient-driven modes and anomalous ion transport in tokamaks](#)

[Physics of Fluids B: Plasma Physics](#) **1**, 1018 (1989); <https://doi.org/10.1063/1.859023>

[Critical gradient formula for toroidal electron temperature gradient modes](#)

[Physics of Plasmas](#) **8**, 4096 (2001); <https://doi.org/10.1063/1.1391261>

[Toroidal drift modes driven by ion pressure gradients](#)

[The Physics of Fluids](#) **24**, 1077 (1981); <https://doi.org/10.1063/1.863486>

[Collisionless electron temperature gradient instability](#)

[The Physics of Fluids](#) **30**, 1331 (1987); <https://doi.org/10.1063/1.866248>

[Gyrokinetic simulation of collisionless trapped-electron mode turbulence](#)

[Physics of Plasmas](#) **12**, 072309 (2005); <https://doi.org/10.1063/1.1947447>

Toroidal electron temperature gradient driven drift modes

W. Horton and B. G. Hong

Institute for Fusion Studies, The University of Texas at Austin, Austin, Texas 78712

W. M. Tang

Plasma Physics Laboratory, Princeton University, Princeton, New Jersey 08540

(Received 14 March 1988; accepted 30 June 1988)

The electron temperature gradient in tokamak geometry is shown to drive a short wavelength lower hybrid drift wave turbulence resulting from the unfavorable magnetic curvature on the outside of the torus. Ballooning mode theory is used to determine the stability regimes and the complex eigenfrequencies. At wavelengths of the order of the electron gyroradius, the polarization is electrostatic and the growth rate is greater than the electron transit time around the torus. At longer wavelengths of the order of the collisionless skin depth, the polarization is electromagnetic with electromagnetic vortices producing the dominant transport. The small scale electrostatic component of the turbulence produces a small, of order $(m_e/m_i)^{1/2}$, drift wave anomalous transport of both the trapped and passing electrons while the c/ω_{pe} scale turbulence produces a neo-Alcator [Nucl. Fusion **25**, 1127 (1985)] type transport from the stochastic diffusion of the trapped electrons.

I. INTRODUCTION

The electron temperature gradient in tokamaks has long been recognized as a source of free energy available to drive the collective drift modes unstable while producing an anomalous transport of particles and, in particular, the anomalous electron thermal flux^{1,2} across the confining magnetic field. For the low frequency electron drift wave, the destabilization by the electron temperature gradient in the dissipative trapped electron regime is well known and has been developed as a model for explaining the anomalous electron transport in tokamaks. Less theoretical attention, however, has been given to the higher frequency lower hybrid drift wave, which can also be destabilized by the electron temperature gradient. Recently, Guzdar *et al.*³ have proposed that it is the lower hybrid drift mode driven by the electron temperature gradient and magnetic shear that may be responsible for a substantial anomalous electron transport. The linear theory for a sheared slab with the η_e driven lower hybrid instability is given by Lee *et al.*⁴

In the present work we argue that it is a toroidal version of the lower hybrid drift mode driven unstable by charge separation as a result of the unfavorable grad B and curvature electron drifts in the presence of the electron temperature gradient that may drive this form of short wavelength drift wave turbulence in tokamaks. Ballooning mode formalism is used to examine both the hydrodynamic and the kinetic theory of these instabilities. The local hydrodynamic and kinetic dispersion relations are used to derive the threshold for instability and the parametric dependence of the growth rates.

In the nonlinear regime we recognize that the turbulence problem contains two space scales. At the short wavelengths, where the maximum linear growth rate pumps energy into the electrostatic turbulence, the reduced equations have essentially the same form as those governing the electrostatic η_i mode turbulence with an appropriate interchange of the ion and electron dynamics. Results from the η_i studies⁵⁻¹⁰ show that the fluctuation spectrum mode couples

energy to larger scale fluctuations with spectral index of about 3 in the appropriate range of k space. For the η_e mode, this inverse cascade, or mode coupling to larger space scales, drives a coupling to $A_{||}$ fluctuations at the scale c/ω_{pe} .

At the larger space scales on the order of the collisionless skin depth, c/ω_{pe} , the fluctuations become neutrally stable electromagnetic vortices with small $k_{||}$. This driven secondary electromagnetic turbulence is expected to lead to a large stochastic diffusion of the trapped electrons as shown in the nonlinear transport studies of Horton *et al.*¹¹ and Parail and Yushmanov.¹² The stochastic transport studies indicate that once the turbulence level reaches the mixing length level, the electron diffusivity is insensitive to the details of the fluctuation spectrum and is given by the random walk of the trapped electrons over the correlation length c/ω_{pe} at the rate of the decorrelation frequency, which is of the order of the bounce frequency of the trapped electrons. The stochasticity occurs because of the overlap of the vortex circulation frequency with the parallel bounce frequency. These considerations suggest the conclusions that for electron temperature gradients well above the linear threshold, $\eta_{e,crit} \approx \frac{2}{3}$, the transport may become approximately independent of η_e and be given by the simple stochastic diffusion formula (as studied in Ref. 11) for densities below a critical density. The stochastic diffusion studies show that for the electron density above a critical value, the scale length c/ω_{pe} becomes too small for this component of turbulence to compete with the anomalous transport from the longer wavelength low frequency drift wave turbulence driven principally by the ion temperature gradient.

In Sec. II we analyze the electrostatic toroidal ballooning mode equations. The electromagnetic equations are investigated in Sec. III. In Sec. IV we analyze the reduced nonlinear hydrodynamic equations and their conservation law(s) and discuss the expected turbulence and anomalous transport predicted by this model. Finally, in Sec. V, we summarize the characteristics of the toroidal η_e turbulence and the expected scaling of the anomalous transport. The

absence of an explicitly strong dependence of the diffusivity on the parameter η_e is in marked contrast with the results of Guzdar *et al.*,³ who found $\chi_e \propto \eta_e (1 + \eta_e)$. The signatures of the processes considered are summarized for experimental identification, and we suggest directions for future linear and nonlinear studies of the toroidal η_e turbulence.

II. HYDRODYNAMIC DESCRIPTION OF SHORT WAVELENGTH ∇T_e TURBULENCE

We assume that the dominant part of the toroidal ∇T_e driven turbulence can be taken to fall in the hydrodynamic regime for the electron response functions since $\gamma \sim v_e / (r_T R)^{1/2} > k_{\parallel} v_e$ and $k_{\perp} \rho_e < 1$. We compute the electron density fluctuations from a continuity equation of the form

$$\frac{\partial n_e}{\partial t} + \mathbf{v}_{\perp e} \cdot \nabla n_e + n_e \nabla \cdot \mathbf{v}_{\perp e} + n_e \nabla \cdot \mathbf{v}_p + n_e \nabla_{\parallel} v_{\parallel e} = 0, \quad (1)$$

where the hydrodynamic velocities are given by

$$\mathbf{v}_{\perp e} = (\hat{\mathbf{c}} \times \nabla \Phi) / B + (\hat{\mathbf{c}} \times \nabla p_e) / (-en_e B), \quad (2)$$

$$\mathbf{v}_p = -\frac{m_e c^2}{eB^2} \left(\frac{\partial}{\partial t} + \mathbf{v}_{de} \cdot \nabla \right) \nabla_{\perp} \Phi, \quad (3)$$

and

$$\frac{dv_{\parallel e}}{dt} = \left(\frac{e}{m_e} \right) \hat{\mathbf{b}} \cdot \nabla \Phi - \frac{\hat{\mathbf{b}} \cdot \nabla p_e}{m_e n_e}. \quad (4)$$

In the perpendicular electron momentum balance, Eq. (3), we used the cancellation relation between the electron diamagnetic drift velocity v_{de} and the finite Larmor radius stress tensor. Their nonlinear form is given in Ref. 5. The electron thermal balance is given by

$$\frac{3}{2} \frac{\partial}{\partial t} (n_e T_e) + \nabla \cdot \left(\frac{3}{2} n_e T_e \mathbf{v}_{\perp e} + \mathbf{q}_e \right) + n_e T_e \nabla \cdot \mathbf{v}_{\perp e} = \kappa_{\parallel} \nabla_{\parallel}^2 T_e, \quad (5)$$

where

$$\mathbf{q}_e = \frac{1}{2} (p_e \hat{\mathbf{b}} \times \nabla T_e) / m_e \omega_{ce}$$

and $\kappa_{\parallel} = \alpha n_e T_e / m_e v_e$, with $\alpha = 3.16$. In the thermal balance equation (5) we neglect the effects of the parallel compression and $\nabla \cdot \mathbf{v}_p$. In the limit where the diamagnetic drifts are small compared with the $\mathbf{E} \times \mathbf{B}$ drift and the finite Larmor radius heat flux \mathbf{q}_e is neglected, the thermal balance Eq. (5) reduces to the adiabatic equation of state,

$$\frac{\partial}{\partial t} p_e + \mathbf{v} \cdot \nabla p_e + \Gamma p_e \nabla \cdot \mathbf{v} = 0,$$

with $\Gamma = \frac{5}{3}$.

For the modes of interest here, the appropriate form for the kinetic ion response is

$$\delta n_i = -\frac{n_i e \Phi}{T_i} \left[1 - \left\langle \frac{\omega - \omega_{*i}}{\omega - \omega_{Di}} J_0^2 \left(\frac{k_{\perp} v_{\perp}}{\omega_{ci}} \right) \right\rangle \right], \quad (6)$$

$$\cong - (n_i e \Phi / T_i) (1 - i \delta_i), \quad (7)$$

where δ_i is a small resonant contribution that occurs for modes rotating in the ω_{Di} direction, with ω_{Di} being the ion

grad B and curvature drift frequency. The adiabatic ion response in Eq. (7) follows in fluid theory from the balance, $e_i n_i \mathbf{E} = -e_i n_i \nabla \Phi = \nabla p_i = T_i \nabla \delta n_i$.

We now consider ballooning-type modes in the usual circular cross-section tokamak with $B_T = B_0 / (1 + \epsilon \cos \theta)$ and $B_{\theta} = (\epsilon / q) B_T$, where $\epsilon = r / R$ and $q(r) = rB / RB_{\theta}$. The density, temperature, and potential fluctuations are taken to vary as

$$f = f(r) + \delta f(\theta) e^{il[q(r)\theta - \phi] - i\omega t} + \text{c.c.} \quad (8)$$

This mode gives rise to $k_{\perp}^2 = k_{\theta}^2 (1 + s^2 \theta^2)$ with $k_{\theta} = lq / r$ and the parallel derivative $i k_{\parallel} = (1 / qR) \partial / \partial \theta$.

In this geometry, where $\nabla(1/B^2) = 2\hat{\mathbf{x}}/B^2 R$, the fluid compression terms in Eqs. (1) and (5) are computed to give

$$\begin{aligned} \nabla \cdot \mathbf{v}_{de} &= -\frac{\hat{\mathbf{c}} \times \nabla p_e}{en_e B} \cdot \left(\frac{2\hat{\mathbf{x}}}{R} + \frac{\nabla n_e}{n_e} \right) \\ &= \frac{\mathbf{v}_{De}}{p_e} \cdot \nabla p_e + \frac{\mathbf{v}_{de}}{T_e} \cdot \nabla T_e, \end{aligned} \quad (9)$$

$$\nabla \cdot \mathbf{v}_E = - (e / T_e) \nabla_{De} \cdot \nabla \Phi,$$

$$\nabla \cdot (n \mathbf{v}_{de}) = (\mathbf{v}_{De} / T_e) \cdot \nabla p_e,$$

where

$$\mathbf{v}_{De} = (2cT_e / eBR) \hat{\mathbf{b}} \times \hat{\mathbf{x}} \text{ and } \mathbf{v}_{de} = -(\hat{\mathbf{c}} \times \nabla p_e) / eBn_e, \quad (10)$$

with $\hat{\mathbf{x}} = \nabla x = \nabla(r \cos \theta)$. Similarly, the divergence of \mathbf{q}_e reduces to

$$\nabla \cdot \mathbf{q}_e = \frac{1}{2} n \mathbf{v}_{De} \cdot \nabla T_e - \frac{1}{2} n \mathbf{v}_{de} \cdot \nabla T_e, \quad (11)$$

where the first term cancels parts of the \mathbf{v}_{de} contributions in Eq. (5). With Eqs. (9)–(11), the thermal balance Eq. (5) reduces to

$$\begin{aligned} \frac{\partial p_e}{\partial t} + \mathbf{v}_E \cdot \nabla p_e + \Gamma p_e \nabla \cdot \mathbf{v}_E + \Gamma \mathbf{v}_{De} \cdot \nabla p_e + \Gamma n_e \mathbf{v}_{De} \cdot \nabla T_e \\ = \frac{3}{2} \kappa_{\parallel} \nabla_{\parallel}^2 T_e. \end{aligned}$$

The results from Eqs. (8)–(11) are used along with the following definitions:

$$\begin{aligned} \omega_{*e} &= \mathbf{k} \cdot \mathbf{v}_{de} = -k_{\theta} \frac{cT_e}{eBn_e} \frac{dn_e}{dr}, \\ \omega_{*pe} &= (1 + \eta_e) \omega_{*e}, \\ \omega_{De} &= \mathbf{k} \cdot \mathbf{v}_{De} = k_{\theta} (2cT_e / eBR) g(\theta), \end{aligned} \quad (12)$$

and

$$g(\theta) = \cos \theta + s \theta \sin \theta.$$

We obtain from linearizing Eqs. (1) and (5) and using Eqs. (9)–(12):

$$\begin{aligned} -i\omega \frac{\delta n_e}{n_e} + i(\omega_{*e} - \omega_{De}) \frac{e\Phi}{T_e} \\ + i\omega_{De} \frac{\delta p_e}{p_e} + ik_{\perp}^2 \rho_e^2 (\omega - \omega_{*pe}) \frac{e\Phi}{T_e} \\ - i \frac{k_{\parallel}^2 v_e^2}{\omega} \left(\frac{e\Phi}{T_e} - \frac{\delta p_e}{p_e} \right) = 0, \end{aligned} \quad (13)$$

and

$$-i\omega \frac{\delta p_e}{p_e} + i\omega_{*pe} \frac{e\Phi}{T_e} + i\Gamma \left(\omega \frac{\delta n_e}{n_e} - \omega_{*e} \frac{e\Phi}{T_e} \right) + i\Gamma \omega_{De} \left(\frac{\delta p_e}{p_e} - \frac{\delta n_e}{n_e} \right) = 0. \quad (14)$$

Solving Eqs. (13) and (14) for δn_e and δp_e , as functions of Φ , gives

$$\frac{\delta n_e}{n_e} = \frac{\omega_{*e} - \omega_{De} + k_{\perp}^2 \rho_e^2 (\omega - \omega_{*pe}) - k_{\parallel}^2 v_e^2 / \omega + (\omega_{De} + k_{\parallel}^2 v_e^2 / \omega) [\omega_{*e} (\eta_e + 1 - \Gamma) / (\omega - \Gamma \omega_{De})]}{\omega - \Gamma (\omega_{De} + k_{\parallel}^2 v_e^2 / \omega) [(\omega - \omega_{De}) / (\omega - \Gamma \omega_{De})]} \left(\frac{e\Phi}{T_e} \right), \quad (15)$$

$$\frac{\delta p_e}{p_e} = \frac{\Gamma (\omega - \omega_{De}) [\omega_{*e} - \omega_{De} + k_{\perp}^2 \rho_e^2 (\omega - \omega_{*pe}) - k_{\parallel}^2 v_e^2 / \omega] + \omega \omega_{*e} (\eta_e + 1 - \Gamma)}{\omega (\omega - \Gamma \omega_{De}) - \Gamma (\omega_{De} + k_{\parallel}^2 v_e^2 / \omega) (\omega - \omega_{De})} \left(\frac{e\Phi}{T_e} \right), \quad (16)$$

where we consider $k_{\parallel}^2 \kappa_{ie} \lesssim k_{\parallel} v_e \ll \omega$ in writing Eq. (16).

The density and temperature fluctuations (15) and (16) reduce in the magnetohydrodynamic (MHD) limit $|\omega| \gg \omega_{*e}, \omega_{De}$ to

$$\frac{\delta n_e}{n_e} \cong \left[\frac{\omega_{*e}}{\omega} - \frac{\omega_{De}}{\omega} \left(1 - \frac{\omega_{*pe}}{\omega} \right) + k_{\perp}^2 \rho_e^2 \left(1 - \frac{\omega_{*pe}}{\omega} \right) - \frac{k_{\parallel}^2 v_e^2}{\omega^2} \left(1 - \frac{\omega_{*pe}}{\omega} \right) \right] \left(\frac{e\Phi}{T_e} \right),$$

$$\frac{\delta p_e}{p_e} \cong \left(\frac{\omega_{*pe}}{\omega} - \Gamma \frac{\omega_{De}}{\omega} \right) \left(\frac{e\Phi}{T_e} \right).$$

In the earlier work on the toroidal ∇T_i modes, the ion pressure fluctuations were taken in the incompressible convective limit where $\delta p_i / p_i \cong -(\omega_{*pi} / \omega) (e_j \Phi / T_j)$. The present work includes the fluid compressional effects from the many terms given in Eqs. (15) and (16). Recently, Jarman *et al.*¹⁰ have also derived the η_i -mode equations with these thermal compressional terms in a hydrodynamic description.

We use Eqs. (7) and (15) to compute the charge density fluctuations for Poisson's equation in the ballooning mode approximation. After some algebra we obtain

$$\begin{aligned} & \left[\frac{\omega_{*e}}{\tau} (\eta_e + 1 - \Gamma) + \Gamma \left(1 + \frac{1}{\tau} \right) \omega_{De} - \left(\Gamma + \frac{1}{\tau} \right) \omega \right] \\ & \times \frac{v_e^2}{\omega^2 q^2 R^2} \frac{d^2 \Phi(\theta)}{d\theta^2} - \left\{ \left(1 + \frac{k_{\perp}^2 \rho_e^2}{\tau} + k^2 \lambda_{Di}^2 - i\delta_i \right) \omega \right. \\ & + \left[\frac{\omega_{*e}}{\tau} - \frac{\omega_{*pe}}{\tau} k_{\perp}^2 \rho_e^2 - \left(2\Gamma + \frac{1}{\tau} \right) \omega_{De} \right. \\ & - \Gamma \frac{\omega_{De}}{\tau} k_{\perp}^2 \rho_e^2 \left. \right] + \frac{\omega_{*e} \omega_{De}}{\tau \omega} \left(\eta_e - \frac{2}{3} - \Gamma \right) \\ & \left. + \Gamma \left(1 + \frac{1}{\tau} \right) \frac{\omega_{De}^2}{\omega} + \Gamma \frac{\omega_{*De} \omega_{*pe}}{\tau \omega} k_{\perp}^2 \rho_e^2 \right\} \Phi(\theta) = 0. \end{aligned} \quad (17)$$

Equation (17) describes the propagation of the lower hybrid drift mode in toroidal geometry. Using the local approximation and taking $\omega_{De} / \omega_{*e} = 2\epsilon_n \ll 1$, the frequency of the mode is

$$\omega \cong \omega_{*i} [1 - (1 + \eta_e) k_{\perp}^2 \rho_e^2] / (1 + k_{\perp}^2 \rho_e^2 d_e / \tau - i\delta_i), \quad (18)$$

where $\omega_{*i} = -\omega_{*e} / \tau$ and $d_e = 1 + \omega_{ce}^2 / \omega_{pe}^2$. For increasing η_e , the frequency (18) of the lower hybrid mode decreases until it couples with the toroidal drift frequency $\omega_{De}(\theta)$. The coupling produces a destabilizing charge separation on the outside of the torus where $\omega_{*pe} \omega_{De}(\theta) > 0$. The coupling of the lower hybrid drift to ω_{De} is strongest where the coefficient of the terms independent of ω in the square bracket in Eq. (17) vanishes. Physically, this is where the phase velocity of the mode in Eq. (18) is vanishing. In this range of k the local dispersion relation gives

$$\gamma^2 = -\omega^2 \cong \omega_{*e} \omega_{De}(\theta) (\eta_e + 1 - \Gamma) / (\tau + k^2 \rho_e^2 d_e). \quad (19)$$

We now consider the instability domain and the characteristic growth rates in both the local limit and as determined by the ballooning mode Eq. (17).

A. Local approximation

The unstable eigenmodes are localized to the outside of the torus with $\Phi(\theta) \sim \exp(-\sigma_k \theta^2 / 2)$. For $\text{Re } \sigma_k > 1$ the mode frequency and growth rate are given to the first order by dropping the $v_e^2 / \omega^2 q^2 R^2$ term in Eq. (17) and evaluating the toroidal drift terms at $\theta = 0$. In this limit the dispersion relation becomes the quadratic equation

$$\begin{aligned} & (1 + k_{\perp}^2 \rho_{ei}^2 d_e) \omega^2 + (\omega / \tau) [\omega_{*e} - \omega_{De} (1 + 2\tau \Gamma) \\ & - \omega_{*pe} k_{\perp}^2 \rho_e^2 - \Gamma \omega_{De} k_{\perp}^2 \rho_e^2] \\ & + (\omega_{De} \omega_{*e} / \tau) (\eta_e + 1 - \Gamma) \\ & - (\Gamma / \tau) \omega_{*e} \omega_{De} + \Gamma (1 + 1/\tau) \omega_{De}^2 \\ & + \Gamma k_{\perp}^2 \rho_{ei}^2 \omega_{*pe} \omega_{De} = 0. \end{aligned} \quad (20)$$

In Eq. (20) and the following it is useful to introduce the natural dimensionless variables for the mode by the following definitions:

$$v_{ei} = (T_i / m_e)^{1/2}, \quad \rho_{ei} = v_{ei} / \omega_{ce} = c(m_e T_i)^{1/2} / eB, \\ k = k \rho_{ei}.$$

We measure frequencies in units of v_{ei} / r_n so that

$$\omega_{*e} = (\tau k \rho_{ei} v_{ei} / r_n) \rightarrow \tau k, \quad \omega_{*i} = -k (v_{ei} / r_n) \rightarrow -k \\ \text{and} \\ \omega_{De} \rightarrow 2\epsilon_n \tau k, \quad \omega_{*pe} \rightarrow \tau k (1 + \eta_e), \quad (21)$$

where

$$\epsilon_n = \frac{r_n}{R} \quad \text{and} \quad \eta_e = \frac{d \ln T_e}{d \ln n_e} = \frac{r_n}{r_{Te}}.$$

In these units the dispersion relation becomes

$$A\omega^2 + B\omega + C = 0, \quad (22)$$

with

$$\begin{aligned} A &= 1 + k^2 d_e - i\delta_i, \\ B &= ku_k \equiv k \{1 - 2\epsilon_n(1 + 2\Gamma\tau) \\ &\quad - k^2[\tau(1 + \eta_e) + 2\Gamma\tau\epsilon_n]\}, \\ C &= 2\epsilon_n\tau k^2[\eta_e - \frac{2}{3} - \Gamma \\ &\quad + k^2\tau(1 + \eta_e)\Gamma + 2\Gamma\epsilon_n(1 + \tau)]. \end{aligned}$$

The local modes are given by

$$\begin{aligned} \omega_{\pm}^{(0)} &= [k/2(1 + k^2 d_e - i\delta_i)](-u_k \pm \{u_k^2 - 8\tau\epsilon_n \\ &\quad \times [\eta_e - \frac{2}{3} - \Gamma + \Gamma\tau k^2(1 + \eta_e) \\ &\quad + 2\Gamma\epsilon_n(1 + \tau)](1 + k^2 d_e - i\delta_i)\}^{1/2}) \end{aligned} \quad (23)$$

in units of v_{ei}/r_n . The maximum growth rate γ_m occurs at $k = k_m$, where $u_k^2 \rightarrow 0$, which gives

$$\begin{aligned} k_m &= \{[1 - 2\epsilon_n(1 + 2\Gamma\tau)]/[\tau(1 + \eta_e) + 2\Gamma\tau\epsilon_n]\}^{1/2} \\ &< 1. \end{aligned} \quad (24)$$

For $k \sim k_m$ the growth rate is

$$\begin{aligned} \gamma_m &\simeq k_m(2\epsilon_n\tau)^{1/2}[\eta_e - \frac{2}{3} - \Gamma + 2\Gamma\epsilon_n(1 + \tau) \\ &\quad + \Gamma k_m^2\tau(1 + \eta_e)]^{1/2} \\ &\simeq k_m(2\epsilon_n\tau)^{1/2}(\eta_e + 1 - \Gamma)^{1/2}, \end{aligned} \quad (25)$$

giving

$$\eta_{e,\text{crit}} \simeq \frac{2}{3}$$

as the critical temperature-to-density gradient ratio for instability. A more precise condition follows from examining $B^2 = 4AC$ using coefficients (22). This condition gives the approximate critical value

$$\begin{aligned} \eta_{e,\text{crit}} &= \frac{2}{3} + \Gamma - 2\Gamma\epsilon_n(1 + \tau) - \Gamma(1 + \eta_e) \\ &\quad \times \{[1 - 2\epsilon_n(1 + 2\Gamma\tau)]/(1 + \eta_e + 2\Gamma\epsilon_n)\}. \end{aligned} \quad (26)$$

For $\eta_e \gg \eta_{e,\text{crit}}$, the maximum growth rate varies as

$$\gamma_m \simeq (2\epsilon_n)^{1/2}(v_{ei}/r_n), \quad (27)$$

valid for $\epsilon_n < 1$.

For flat density profiles where $\epsilon_n \gtrsim 1$ it is important to redefine the dimensionless frequencies with $v_{ei}/r_n \rightarrow v_{ei}/r_{Te}$. Then the instability exists for $r_n \rightarrow \infty$ with the frequencies

$$\begin{aligned} \omega_{\pm} &= [k/2(1 + k^2 d_e)](u_k^{\infty} \pm \{(u_k^{\infty})^2 - 8\tau\epsilon_n \\ &\quad \times [1 + \Gamma k^2\tau + 2\Gamma\epsilon_n(1 + \tau)](1 + k^2 d_e)\}^{1/2}) \end{aligned} \quad (28)$$

(in units of v_{ei}/r_T), where

$$u_k^{\infty} = 2\epsilon_n(1 + 2\Gamma\tau + \Gamma\tau k^2) + k^2\tau.$$

Examining $B^2 = 4AC$ leads to the unstable domain

$$\frac{-x_1 - \sqrt{x_1^2 - x_2}}{R} < \frac{1}{r_{Te}} < \frac{-x_1 + \sqrt{x_1^2 - x_2}}{R}, \quad (29)$$

where

$$\begin{aligned} x_1 &= (4/k^4\tau)(1 + k^2 d_e)(1 + \Gamma\tau k^2) \\ &\quad - (2/k^2\tau)(1 + 2\Gamma\tau + \Gamma\tau k^2), \\ x_2 &= (4/k^4\tau^2)(1 + 2\Gamma\tau + \Gamma\tau k^2)^2 \\ &\quad - [16\Gamma(1 + \tau)/k^4\tau](1 + k^2 d_e). \end{aligned} \quad (30)$$

The condition (29) is similar to that given by Jarmén *et al.*¹⁰ for the η_i mode where, however, the study is restricted to $\epsilon_n < \frac{1}{4}$. The stabilizing effect of compressibility is also studied by Dominguez and Moore.¹³

In Fig. 1 we show the domain of instability in the r_{Te} - r_n parameter space at fixed k . There are onset thresholds required by Eq. (29) for finite bad curvature and cutoff values at large ϵ_n because of compressional stabilization. The threshold at $\eta_e = \frac{2}{3}$ is clearly shown for the system without the finite Larmor radius (FLR) heat flux, but the threshold is moved to $\eta_e < 1$ when the FLR heat flux is included.

The stability conditions for $r_n \gg r_{Te}$ are relevant to auxiliary-heated divertor tokamak discharges which exhibit improved ("H-mode type") confinement properties.¹⁴ With the exception of the edge region, the characteristic density profiles tend to be relatively flat. Even though there can be a factor of 2 to 4 improvement in the energy confinement time for such plasmas, the electron thermal transport nevertheless remains anomalously large by at least two orders of mag-

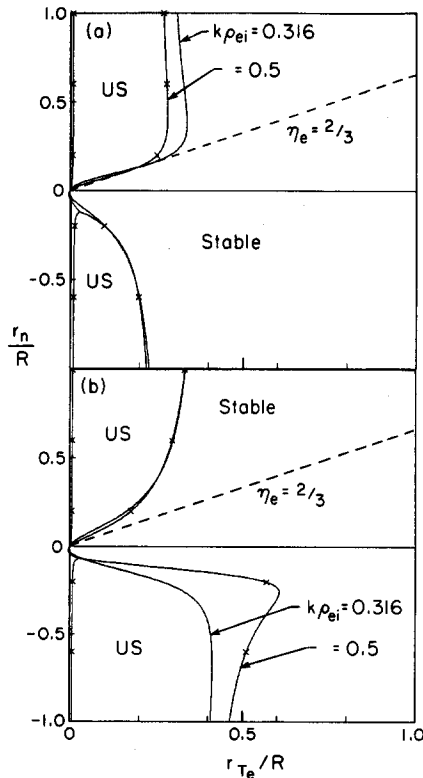


FIG. 1. Stable (S) and unstable (US) domains in the r_{Te} - r_n parameter space at two values of $k = k_{lei}$. The dispersion relation in part (a) neglects the FLR electron heat flux and part (b) includes the FLR heat flux.

nitude over neoclassical estimates. Previous studies have demonstrated that even in the limit of zero density gradient, low frequency microinstabilities can persist because of the nonzero temperature gradient.¹⁵ The unstable η_i -mode domain for flat density profiles is given by Dominguez and Waltz for hydrodynamic equations neglecting the FLR heat flux.¹⁶ The weaker overall pressure gradients in the interior region of the H-mode plasmas do lead to correspondingly smaller values of the electron thermal diffusivity, which is in turn consistent with the observed improvement in the energy confinement time. With respect to the relatively high frequency toroidal electron temperature gradient driven drift modes analyzed in the present work, the fastest growing mode for the flat density gradient limit, $\eta_e \rightarrow \infty$, occurs for

$$k_m^\infty \approx (2\epsilon_T/\tau)^{1/2}, \quad (31)$$

with

$$\gamma_m^\infty = k_m (2\epsilon_T\tau)^{1/2} = 2\epsilon_T(v_{ei}/r_T) = 2v_{ei}/R, \quad (32)$$

which is greater than $k_\parallel^0 v_e = v_e/qR$ for $(T_i/T_e)^{1/2} > 1/2q$. At fixed $k > \tau\epsilon_T^{1/2}/q$ as required by $\gamma_k > k_\parallel v_e$, the growth rate scales as $\gamma = kv_{ei}/(r_{Te}R)^{1/2}$.

For local theory we can compare the results of the hydrodynamic dispersion relation with the Vlasov kinetic theory dispersion relation using the guiding center dispersion function

$$P(\omega, k, \eta_e, \epsilon_n) = \left\langle \frac{[\omega - \omega_{*e}(v^2)] J_0^2(k_\parallel v_\parallel / \omega_{ce})}{\omega - \omega_{De}(\frac{1}{2}v_\perp^2 + v_\parallel^2)/v_e^2} \right\rangle_{MB} \quad (33)$$

The electrostatic dispersion relation is

$$D = 1 + k^2 \lambda_{Di}^2 + 1/\tau [1 - P_e(\omega, k, \eta_e, \epsilon_n)]. \quad (34)$$

Using Nyquist stability diagrams we find that for small $k < 0.5$, the condition for instability $\eta_e > \eta_{e,crit}$ obtained from $\text{Im } D(\omega) = 0$ is that

$$\eta_e > \eta_{e,crit} = \frac{2}{3}. \quad (35)$$

When the condition given by Eq. (35) is satisfied, the wave-particle resonance produces an unstable sign of $\text{Im } D < 0$ for $\omega > 0$ for positive energy modes. The condition for accessibility of the temperature gradient free energy to the wave requires that $\text{Re } D(\omega_m) < 0$, where $\omega_m \approx 2\epsilon_n k \times (1 - 3\eta_e/2)/(2\epsilon_n - \eta_e)$ is the frequency where $\text{Im } D_{es}(\omega_m) = 0$. Evaluating $\text{Re } D(\omega_m)$ leads to the condition

$$\epsilon_T = r_{Te}/R < 0.7/(1 + \tau + k^2 \lambda_{Di}^2), \quad (36)$$

when $\eta_e > \frac{2}{3}$ for unstable modes. The Nyquist diagrams are shown in Fig. 2. At marginal stability the mode frequency is near zero for $k \lesssim 0.5$. Resonant thermal electrons are involved in the kinetic dispersion relation. The wave phase velocity $\omega_k/2k\epsilon_n \approx (\frac{2}{3} - \eta_e^{-1})$ determines the resonant ellipse in velocity space through

$$(\frac{1}{2}v_\perp^2 + v_\parallel^2)/v_e^2 = \omega_k/2k\epsilon_n. \quad (37)$$

The strength of the resonance vanishes as $\text{Im } P_e \approx (\omega/2k\epsilon_n)^{1/2}$ as $\omega/2k\epsilon_n \rightarrow 0^+$.

Thus in toroidal geometry the resonant electrons deter-

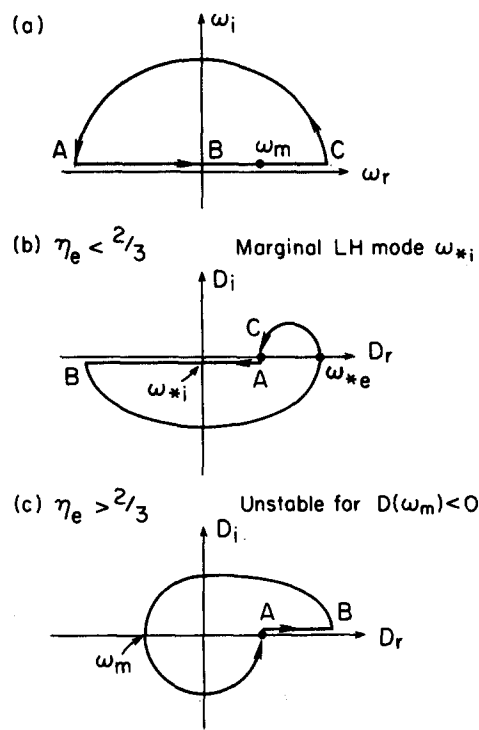


FIG. 2. Nyquist diagram of the kinetic dispersion relation above and below the critical η_e value.

mining stability and the anomalous transport are the thermal electrons. Only for $\epsilon_n \rightarrow 0$, where $\omega_k/2k\epsilon_n \rightarrow 1/\epsilon_n^{1/2} \gg 1$, is the resonance limited to high energy electrons. In slab geometry the resonance occurs for $v_\perp \sim v_e$ but only for a given $v_\parallel = \omega/k_\parallel^0 \gg v_e$, which substantially reduces the number of resonant electrons.

In Figs. 3 and 4 local electrostatic kinetic theory parametric dependence of the toroidal η_e instability is given. In Fig. 2 the growth rate is shown to onset at $\eta_e = \frac{2}{3}$ for small k and closer to $\eta_e = 1$ for $k = 0.5$. Above the threshold in η_e the growth rate increases as $\gamma \sim 0.1v_{ei}/r_{Te} = 0.1\eta_e(v_{ei}/r_n)$ for $k \gtrsim 0.3$. The frequency of the mode changes from rotation in the ion diamagnetic direction for $\eta < \frac{2}{3}$ to rotation in the

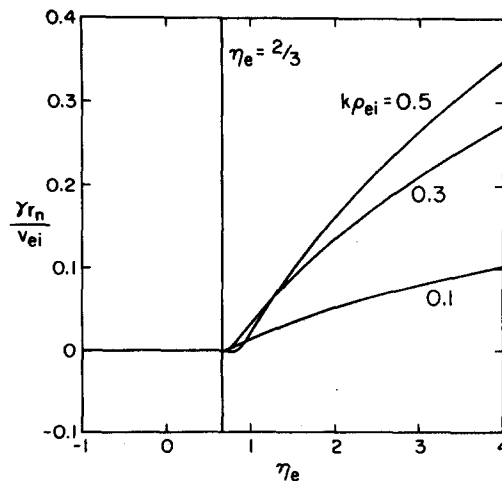


FIG. 3. Kinetic mode growth rate from the local ($\theta = 0$) dispersion relation versus the temperature gradient parameter.

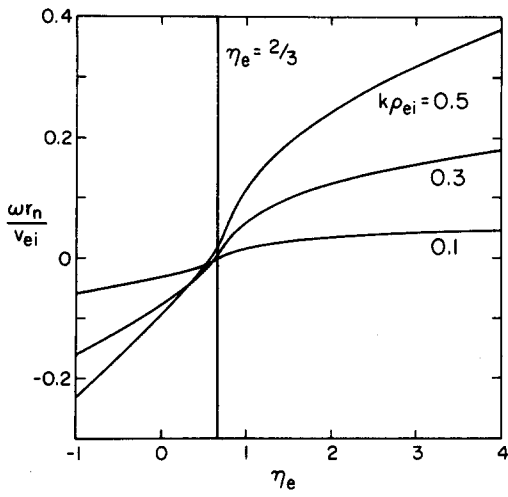


FIG. 4. Kinetic mode frequency corresponding to the growth rate in Fig. 2. Positive frequencies rotate in the electron diamagnetic direction.

electron direction for $\eta_e > \frac{2}{3}$. Well above threshold there is less than one oscillation ($\omega/\gamma < 2\pi$) in each e -folding. In Fig. 5 the toroidicity parameter is varied at fixed $\eta_e = r_n/r_{Te}$. The instability requires fixed $\eta_e = r_n/r_{Te}$. The instability requires finite toroidicity and then is stabilized by compression for $\epsilon_n > \epsilon_n^{\text{crit}}(\eta_e)$ as described in Fig. 1 with fluid theory. There is good agreement between fluid theory and kinetic theory with the FLR heat flux required to explain the kinetic theory results for $k \gtrsim 0.3$. [The $\gamma(k), \omega(k)$ curves not given here are similar to those obtained from Eq. (22) with the usual kinetic theory reduction of γ_{max} and broadening in wavenumber range.] Since thermal electrons are resonant at marginal stability, the hydrodynamic dispersion relations do not predict accurately the conditions for marginal instability as is well known for η_i modes. Now we consider the effect of magnetic shear and the averaging of $\omega_{De}(\theta)$ over the eigenmode wavefunction.

B. Ballooning mode dispersion relation

The analysis of the η_e ballooning problem is similar to that in Refs. 6–8 for the η_i mode. We look for modes localized to along the magnetic field to the outside of the torus,

$$\Phi(\theta) = \Phi_0 \exp(-\sigma_k \theta^2/2), \quad (38)$$

with complex σ_k . From Eq. (17) we obtain

$$\sigma(\omega, k) = \frac{-i\omega q}{\epsilon_n} \left\{ k^2 s^2 \omega \left(d_e - \frac{\tau k(1 + \eta_e)}{\omega} \right) + 2k\epsilon_n \left(\frac{1}{2} - s \right) \left[1 + 2\Gamma\tau - \frac{\tau k}{\omega} \left(\eta_e - \frac{2}{3} - \Gamma \right) \right] \right\}$$

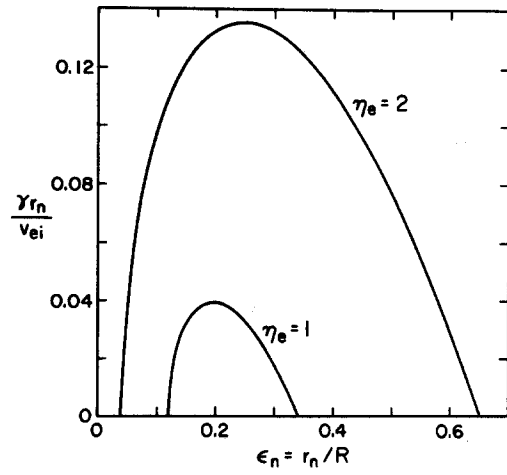


FIG. 5. Kinetic theory growth rate as a function of ϵ_n for fixed η_e and $k\rho_{ei} = 0.3$.

$$\begin{aligned} & - (1 + \tau) \frac{4\Gamma\tau^2 k \epsilon_n}{\omega} \Big] \\ & + 2\Gamma\epsilon_n k^3 \tau \left(s^2 + s - \frac{1}{2} \right) \left(\frac{\tau k(1 + \eta_e)}{\omega} - 1 \right) \Big]^{1/2} \\ & \times \{ [(1 + \Gamma\tau)\omega - k\tau(\eta_e + 1 - \Gamma)]^{1/2} \}^{-1}. \end{aligned} \quad (39)$$

Since $\sigma(\omega, k)$ is complicated, we consider here the limiting form for $|\omega| \ll \omega_{*Te}$ and $ks > (2\epsilon_n)^{1/2}$ leading to

$$\sigma \simeq -i\omega qs |k| / \epsilon_n (1 + \Gamma\tau)^{1/2} \simeq qs |k| \gamma_k / \epsilon_n (1 + \Gamma\tau)^{1/2}. \quad (40)$$

For modes with $\eta_e \gg \frac{2}{3}$ and $k < 1$ the hydrodynamic growth rate is $\gamma_k \simeq |k| (2\epsilon_n \eta_e)^{1/2}$ for $s < 2q$, giving $\sigma_k \simeq k^2 qs (2\eta_e / \epsilon_n)^{1/2}$, requiring $k > k_c \sim (qs)^{-1/2} (\epsilon_n / 2\eta_e)^{1/4}$ for localization.

The ballooning mode dispersion relation is

$$\begin{aligned} & (1 + k^2 d_e - i\delta_i) \omega^2 + \omega k [1 - k^2 \tau (1 + \eta_e) \\ & - 2\epsilon_n (2\Gamma\tau + 1) - 2\Gamma\epsilon_n k^2 \tau] + 2\epsilon_n \tau k^2 [\eta_e - \frac{2}{3} - \Gamma \\ & + 2\Gamma\epsilon_n (1 + \tau) + \Gamma\tau k^2 (1 + \eta_e)] \\ & = (\epsilon_n^2 \tau \sigma / q^2 \omega) [(\Gamma + 1/\tau)\omega - k(\eta_e + 1 - \Gamma)]. \end{aligned} \quad (41)$$

From Eq. (41) the lower hybrid drift frequency again vanishes at $k \simeq k_m$ given in Eq. (24), giving the maximum growth rate γ_m modified by shear and toroidal mode coupling through σ .

Near k_m the ballooning mode dispersion relation becomes

$$\begin{aligned} \omega^2 &= - \frac{2\tau\epsilon_n k^2 [\eta_e - \frac{2}{3} - \Gamma + 2\Gamma\epsilon_n (1 + \tau) + \Gamma\tau k^2 (1 + \eta_e)] + i[(1 + \Gamma\tau)\omega - k\tau(\eta_e + 1 - \Gamma)]\epsilon_n |k| s/q}{1 + k^2 d_e - i\delta_i} \\ &\simeq -2\tau\epsilon_n k^2 \left[\eta_e + 1 - \Gamma - isg(k)(\eta_e + 1 - \Gamma) \left(\frac{s}{2q} \right) \right], \end{aligned} \quad (42)$$

for $k_m^2 \ll 1$ and neglecting δ_i .

Equation (42) describes the transition from the sheared slab regime to the toroidal regime according to $s > 2q$ and $s < 2q$, respectively. In the toroidal regime $s < 2q$, the growth rate is

$$\gamma_k \approx |k| [2\epsilon_n \tau (\eta_e + 1 - \Gamma)]^{1/2} (v_{ei}/r_n),$$

and in the slab regime $s > 2q$, the complex frequency is

$$\omega_k + i\gamma_k = \frac{1+i}{\sqrt{2}} |k| \left(\frac{\tau \epsilon_n s}{q} \right)^{1/2} (\eta_e + 1 - \Gamma)^{1/2} \left(\frac{v_{ei}}{r_n} \right). \quad (43)$$

The formula in Eq. (43) is comparable to Eq. (7) of Ref. 6 at $k_y^2 \rho_e^2 (1 + \eta_e) \sim 1$, except for the absence of the threshold $\eta_e > \Gamma - 1$ in Ref. 4.

With these results for the toroidal slab eigenmodes we compute the $\langle k_x^2 \rangle$ and $\langle k_{\parallel}^2 \rangle$ according to Eqs. (10) and (12) of Ref. 6.

For the toroidal regime $s < 2q$, we obtain

$$\begin{aligned} \langle k_x^2 \rho_e^2 \rangle &\approx \left(\frac{\tau \epsilon_n}{2\eta_e} \right)^{1/2} \frac{s}{q} = \left(\frac{\tau \epsilon_T}{2} \right)^{1/2} \frac{s}{q}, \\ \left\langle \frac{k_{\parallel}^2 v_e^2}{\gamma^2} \right\rangle &\approx \left(\frac{\tau \epsilon_n}{2\eta_e} \right)^{1/2} \frac{s}{q} = \left(\frac{\tau \epsilon_T}{2} \right)^{1/2} \frac{s}{q}, \end{aligned} \quad (44)$$

giving the condition for validity of the hydrodynamic treatment as $s/q < (\eta_e/2\epsilon_n)^{1/2} = 1/(2\epsilon_T)^{1/2}$. For the slab regime we obtain

$$\begin{aligned} \langle k_x^2 \rho_e^2 \rangle &\approx (\tau \epsilon_n / q \eta_e)^{1/2} = (\tau \epsilon_T / q)^{1/2}, \\ \left\langle \frac{k_{\parallel}^2 v_e^2}{\gamma^2} \right\rangle &\approx \left(\frac{\tau \epsilon_n}{q \eta_e} \right)^{1/2} = \left(\frac{\tau \epsilon_T}{q} \right)^{1/2}. \end{aligned} \quad (45)$$

For strong turbulence we may estimate the anomalous transport by $\gamma/\langle k_x^2 \rangle$. In the toroidal regime we obtain

$$\chi'_{es} = \left(\frac{m_e}{m_i} \right)^{1/2} \left(\frac{2q}{s} \right) \eta_e^{1/2} \frac{\rho_s}{r_n} \frac{c T_i}{e B}, \quad (46)$$

for $\epsilon_n < 1$ and in the limit $\eta_e \gg 1$,

$$\chi'_{es} = \left(\frac{m_e}{m_i} \right)^{1/2} \left(\frac{2q}{s} \right) (2\epsilon_T)^{1/2} \frac{\rho_s}{r_T} \frac{c T_i}{e B}. \quad (47)$$

We note that even in the sheared slab regime our formula (46) differs from that of Lee *et al.*,⁴ where $\chi_{Lee} \propto \eta_e (1 + \eta_e)$. The factor $1 + \eta_e$ apparently results when compressional terms are neglected in the thermal balance equation, and the extra unexplained factor of η_e seems to be used as a fit to the specific numerical results from their analysis of the sheared slab eigenvalue equation.

III. ELECTROMAGNETIC FLUCTUATIONS

The long wavelength part of the spectrum derived in Sec. II develops an electromagnetic component described by the parallel vector potential A_{\parallel} . In this section we first estimate the wavenumber for the change of E_{\parallel} from its electrostatic value, and then we derive the electromagnetic ballooning mode equation ignoring magnetic compressibility δB_{\parallel} .

For fluctuations with $\omega > k_{\parallel} v_e$ the parallel conductivity is

$$\sigma_{\parallel}^e = (in_e e^2 / m_e \omega) (1 - \omega_{*pe} / \omega). \quad (48)$$

Using $j_{\parallel} = \sigma_{\parallel}^e E_{\parallel}$ with $\hat{\mathbf{b}} \cdot \nabla \times \mathbf{B} = 4\pi j_{\parallel} / c$ for the electromagnetic fields

$$\mathbf{E} = -\nabla \Phi + (i\omega/c) A_{\parallel} \hat{\mathbf{b}} \quad \text{and} \quad \mathbf{B} = \nabla A_{\parallel} \times \hat{\mathbf{b}}, \quad (49)$$

one obtains for A_{\parallel}

$$\left[\nabla_{\perp}^2 - \frac{\omega_{pe}^2}{c^2} \left(1 - \frac{\omega_{*pe}}{\omega} \right) \right] A_{\parallel} = -\frac{\omega_{pe}^2}{c^2} \left(1 - \frac{\omega_{*pe}}{\omega} \right) \frac{ck_{\parallel} \Phi}{\omega}. \quad (50)$$

Using (50) to calculate A_{\parallel} and then E_{\parallel} we obtain

$$E_{\parallel} = -ik_{\parallel} \Phi k_{\perp}^2 / [k_{\perp}^2 + k_s^2(\omega, k)], \quad (51)$$

with

$$k_s^2 = \frac{\omega_{pe}^2}{c^2} \left(1 - \frac{\omega_{*pe}}{\omega} \right) \approx \frac{i\omega_{pe}^2}{c^2} \left(\frac{\eta_e}{2\epsilon_n} \right)^{1/2}, \quad (52)$$

where we use $\omega \approx i\gamma_k$ given in Eq. (25) for the last estimate. From Eqs. (51) and (52) we find that the electromagnetic shielding of $-ik_{\parallel} \Phi$ is strong for $k \leq k_s$, where

$$k_s = (k_{\perp} \rho_e)_s = \left(\frac{\beta_e}{2} \right)^{1/2} \left(\frac{\eta_e}{2\epsilon_n} \right)^{1/2} = \left(\frac{\beta_e}{4\epsilon_T} \right)^{1/2}. \quad (53)$$

The shielding at $k = k_s$ is in the regime $\omega_{*e} > v_e/qR$, provided $(\beta_e/4\epsilon_T)^{1/2} > \epsilon_n/q$ or $q^2 \beta_e / \epsilon_n^2 > 4\epsilon_T$. For $\epsilon_n \sim \epsilon \equiv r/R$ the quantity $q^2 \beta_e / \epsilon_n^2$ is the beta poloidal $\beta_{Pe} = 8\pi p_e / B_p^2$. We now consider the full set of electromagnetic equations for these fluctuations in the hydrodynamic approximation for the electrons and the adiabatic approximation for the ions.

A. Nonlinear electromagnetic equations

For the electron dynamics we write the density and pressure as $\bar{n}_e + \tilde{n}_e$ and $\bar{p}_e + \tilde{p}_e$ and the velocity as $v_{\parallel e} = \tilde{v}_{\parallel e}$, where the equilibrium current and its gradient are neglected. Here we define the y, z average of $f(x, y, z, t)$ by

$$\bar{f}(x, t) = \iint \frac{dy dz}{L_y L_z} f(x, y, z, t) = \int \frac{d\theta d\phi}{(2\pi)^2} f(x, \theta, \phi, t).$$

For completeness we write the nonlinear equations here and reduce them further in Sec. IV.

The electron continuity equation is

$$\begin{aligned} \frac{\partial \bar{n}_e}{\partial t} + \mathbf{v}_E \cdot \nabla \bar{n}_e + \mathbf{v}_E \cdot \nabla \tilde{n}_e + n_e \nabla \cdot \mathbf{v}_E + \nabla \cdot (n_e \mathbf{v}_{de}) \\ + n_e \nabla \cdot \mathbf{v}_{pe} + n_e \nabla_{\parallel} v_{\parallel e} = 0. \end{aligned} \quad (54)$$

The parallel momentum balance equation is

$$\begin{aligned} m_e n_e \frac{\partial v_{\parallel e}}{\partial t} + m_e n_e \mathbf{v}_E \cdot \nabla v_{\parallel e} \\ = en_e \left(\hat{\mathbf{b}} \cdot \nabla \Phi + \frac{\tilde{\mathbf{B}}}{B} \cdot \nabla \Phi + \frac{1}{c} \frac{\partial A_{\parallel}}{\partial t} \right) \\ - \hat{\mathbf{b}} \cdot \nabla \tilde{p}_e - \frac{\tilde{\mathbf{B}}}{B} \cdot \nabla (\bar{p}_e + \tilde{p}_e), \end{aligned} \quad (55)$$

where $\hat{\mathbf{b}}$ is the unperturbed unit magnetic field vector. The electron thermal balance equation is

$$\frac{\partial \tilde{p}_e}{\partial t} + \mathbf{v}_E \cdot \nabla \tilde{p}_e + \mathbf{v}_E \cdot \nabla \tilde{p}_e + \Gamma p_e \nabla \cdot \mathbf{v}_E + \Gamma \nabla_{De} \cdot \nabla p_e + \Gamma n_e \nabla_{De} \cdot \nabla \tilde{T}_e + v_{\parallel e} \hat{\mathbf{b}} \cdot \nabla \tilde{p}_e + \Gamma p_e \nabla_{\parallel} v_{\parallel e} = 0. \quad (56)$$

For the ions we take

$$\tilde{n}_i = -(n_i e / T_i) \Phi$$

and rewrite Poisson's equation

$$k_{\perp}^2 \Phi = 4\pi e (\tilde{n}_i - \tilde{n}_e),$$

as

$$(1 + k_{\perp}^2 \lambda_{Di}^2) e \Phi / T_i = \tilde{n}_e / n_e. \quad (57)$$

The parallel component of Ampère's law is

$$\nabla_{\perp}^2 A_{\parallel} = -k_{\perp}^2 A_{\parallel} = (4\pi n_e e / c) v_{\parallel e}. \quad (58)$$

B. Linear electromagnetic fluctuations

Substituting Eqs. (49) into Eqs. (54)–(57) and reducing with formulas (8)–(12), yields the following relations between the ballooning mode fluctuations with $\hat{k}_{\parallel} = -i(qR)^{-1}(\partial/\partial\theta)$:

$$\begin{aligned} \omega \frac{\tilde{n}_e}{n_e} - (\omega_{*e} - \omega_{De}) \left(\frac{e\Phi}{T_e} \right) - \omega_{De} \frac{\tilde{p}_e}{p_e} \\ - k_{\perp}^2 \rho_e^2 (\omega - \omega_{*pe}) \left(\frac{e\Phi}{T_e} \right) + k_{\parallel} v_{\parallel e} = 0, \end{aligned} \quad (59)$$

$$\omega v_{\parallel e} = -v_e^2 \hat{k}_{\parallel} \left(\frac{e\Phi}{T_e} \right) + v_e^2 \hat{k}_{\parallel} \left(\frac{\tilde{p}_e}{p_e} \right) + (\omega - \omega_{*pe}) \left(\frac{eA_{\parallel}}{mc} \right), \quad (60)$$

$$\begin{aligned} \omega \frac{\tilde{p}_e}{p_e} - \omega_{*pe} \left(\frac{e\Phi}{T_e} \right) - \Gamma \left(\omega \frac{\tilde{n}_e}{n_e} - \omega_{*e} \frac{e\Phi}{T_e} \right) \\ - \Gamma \omega_{De} \frac{\tilde{T}_e}{T_e} = 0, \end{aligned} \quad (61)$$

where $\tilde{T}_e / T_e = \tilde{p}_e / p_e - \tilde{n}_e / n_e$.

Eliminating $v_{\parallel e}$ and \tilde{p}_e in Eq. (59) using Eqs. (60) and (61) yields

$$\begin{aligned} \left[-1 + \Gamma \left(\frac{\omega_{De}}{\omega} + \frac{v_e^2 \hat{k}_{\parallel}^2}{\omega^2} \right) \left(\frac{\omega - \omega_{*pe}}{\omega - \omega_{De}} \right) \right] \frac{\tilde{n}_e}{n_e} \\ + \left(1 - \frac{\omega_{*pe}}{\omega} \right) \left(\frac{e \hat{k}_{\parallel} A_{\parallel}}{mc \omega} \right) \\ + \left[\frac{\omega_{*e}}{\omega} - \frac{\omega_{De}}{\omega} + k_{\perp}^2 \rho_e^2 \left(1 - \frac{\omega_{*pe}}{\omega} \right) - \frac{v_e^2 \hat{k}_{\parallel}^2}{\omega^2} \right. \\ \left. + \left(\frac{\omega_{De}}{\omega} + \frac{v_e^2 \hat{k}_{\parallel}^2}{\omega^2} \right) \frac{\omega_{*e} (\eta_e + 1 - \Gamma)}{\omega - \Gamma \omega_{De}} \right] \left(\frac{e\Phi}{T_e} \right) = 0. \end{aligned} \quad (62)$$

Expressing \tilde{p}_e / p_e in Eq. (60) in terms of Φ and A_{\parallel} yields the generalized Ohm's law and parallel conductivity. The resulting expression for $v_{\parallel e}$ leads to a fourth-order system of equations. In the remainder of this section we consider the simplified limit where only the first two terms of Eq. (61) are used to determine the pressure fluctuation

$\tilde{p}_e / p_e = (\omega_{*pe} / \omega) (e\Phi / T_e)$ in Eq. (60). The resulting σ_{\parallel}^e is given in Eq. (48) and gives the A_{\parallel} - Φ relation in Eq. (50) valid for $\eta_e \gg \frac{1}{2}$.

Finally, using Eq. (50) to eliminate A_{\parallel} in Eq. (62) yields the ballooning mode equation

$$\begin{aligned} \frac{v_e^2}{q^2 R^2 \omega^2} \left(1 - \frac{\omega_{*pe}}{\omega} \right) \frac{d}{d\theta} \left(\frac{k_{\perp}^2}{k_{\perp}^2 + (\omega_{pe}^2 / c^2) (1 - \omega_{*pe} / \omega)} \right. \\ \left. \times \frac{d\Phi}{d\theta} \right) + \left[\tau (1 - i\delta_i) + k_{\perp}^2 \lambda_{De}^2 + \frac{\omega_{*e}}{\omega} \right. \\ \left. + \left(1 - \frac{\omega_{*pe}}{\omega} \right) \left(k_{\perp}^2 \rho_e^2 - \frac{\omega_{De}}{\omega} \right) \right] \Phi = 0. \end{aligned} \quad (63)$$

For

$c^2 k_{\perp}^2 / \omega_{pe}^2 = (c^2 \omega_{ce}^2 / v_e^2 \omega_{pe}^2) k^2 (1 + s^2 \theta^2) > |1 - \omega_{*pe} / \omega|$, the ballooning mode equation (63) reduces to the electrostatic ballooning mode Eq. (17). For $c^2 k_{\perp}^2 / \omega_{pe}^2 < |1 - \omega_{*pe} / \omega|$, Eq. (63) reduces to

$$\begin{aligned} \frac{c_{Ae}^2 k^2}{q^2 R^2 \omega^2} \frac{d}{d\theta} \left((1 + s^2 \theta^2) \frac{d\Phi}{d\theta} \right) \\ + \left[1 - \frac{\omega_{*i}}{\omega} + \left(1 - \frac{\omega_{*pe}}{\omega} \right) \left(k^2 (1 + s^2 \theta^2) \right. \right. \\ \left. \left. - \frac{\omega_{De}(\theta)}{\tau \omega} \right) \right] \Phi = 0, \end{aligned} \quad (64)$$

where $c_{Ae}^2 = c^2 \omega_{ce}^2 / \omega_{pe}^2$.

Analysis of Eq. (64) shows modes similar to those in Sec. II, except that the wavefunctions are not as well localized to the outside of the torus, and thus the growth rate γ_k is weak or marginally stable in this longer wavelength regime. We now consider the mode coupling between the two k regions. These marginal stable longer wavelength modes, however, can be driven by mode coupling, $\mathbf{k}_2 = \mathbf{k} - \mathbf{k}_1$, of the shorter wavelength unstable modes.

IV. NONLINEAR EQUATION (MODE COUPLING, SATURATION, AND TRANSPORT)

In this section we give the reduced nonlinear equations that describe the coupling of the short wavelength electrostatic fluctuations to the longer wavelength electromagnetic fluctuations. The long wavelength $k_{\perp} \sim \omega_{pe} / c$ regime is expected to produce the dominant transport. Here we investigate the nonlinear equations analytically reserving for future studies their numerical solution.

First we discuss the magnitudes of the nonlinear terms and the mixing length level of saturation. We note that in the electrostatic limit the equations are the same structure as the toroidal η_i equations where the mixing length level of saturation was shown in Ref. 7.

A. Mixing of the electron pressure

In the nonlinear regime there are two mixing rates: (1) the $\mathbf{E} \times \mathbf{B}$ mixing frequency Ω_E determined by the time for convection around the vortex given by $\Phi_k(x, y)$; and (2) the spatial rate of mixing k_{\parallel}^{η} determined by the distance along

B_0 required for going around the magnetic vortex (or island) given by $A_{\parallel k}(x, y)$. The $E \times B$ mixing rate is given by

$$\Omega_E = (ck_x k_y / B) \Phi_k = (k_x r_n e \Phi_k / T_e) \omega_{*e}, \quad (65)$$

which produces¹³ stochastic $E \times B$ transport at the saturation level $\Omega_E \sim \omega_{*e}$. The magnetic mixing rate is given by

$$k_{\parallel}^{nl} = (k_x k_y / B) A_k, \quad (66)$$

which causes stochastic transport when $k_{\parallel}^{nl} \sim k_{\parallel}^0$. For electromagnetic fluctuations with $E_{\parallel} \simeq 0$ the mixing rates are related by

$$k_{\parallel}^{nl} \simeq k_{\parallel}^0 (\Omega_E / \omega),$$

and the saturation levels $\omega \sim \Omega_E$ and $k_{\parallel}^0 \sim k_{\parallel}^{nl}$ yield the fluctuation amplitudes

$$\frac{e\Phi}{T_e} \sim \frac{1}{k_x r_n} \left| \frac{\omega}{\omega_*} \right|, \quad \frac{\delta B_x}{B} \simeq \frac{k_{\parallel}^0}{k_x}. \quad (67)$$

Studies of test electron orbits in tokamaks with such levels of electromagnetic drift wave fluctuations show global stochasticity with transport well described by the diffusion approximation.

For η_e, ϵ_n well past their threshold values, the linear instability may continue to grow until the mixing rates are sufficiently rapid to eliminate the mean electron pressure gradient over the width π/k_x of the fluctuation. Thus we estimate for the saturated state that

$$\nabla_E \cdot \nabla (\bar{p}_e + \bar{p}_e) \simeq 0, \quad \mathbf{B} \cdot \nabla (\bar{p}_e + \bar{p}_e) \simeq 0, \quad (68)$$

in the strongly turbulent state. Both conditions in Eq. (68) determine the same mixing length level of the pressure fluctuation,

$$\langle \bar{p}_e^2 \rangle^{1/2} = \bar{p}_e = \frac{1}{|k_x|} \left| \frac{dp_e}{dx} \right|. \quad (69)$$

If we assume that the rate of mixing Ω_E saturates when $\Omega_E \sim |\omega_k| \sim \gamma_k$ (consistent with Ref. 11) and the rate of magnetic mixing when $k_{\parallel}^{nl} \simeq k_{\parallel}^0$, then the nonlinear fluctuations are consistent with the quasilinear fluctuation equations (59)–(61). For example, using the first two terms in Eq. (61) and Eq. (69) yields

$$\frac{e\Phi}{T_e} \simeq \frac{\omega}{\omega_{*pe}} \frac{\bar{p}_e}{p_e} = \frac{\gamma_k}{\omega_{*e}} \frac{1}{k_x r_n} \simeq \frac{1}{|k_x|} \left(\frac{2}{R r_T} \right)^{1/2}, \quad (70)$$

consistent with $\Omega_E \simeq \gamma_k$. Using level (70) for Φ and the relation (50) gives for A_{\parallel} ,

$$\begin{aligned} \frac{eA_{\parallel}}{T_e} &\simeq \left| \frac{1 - \omega_{*pe}/\omega}{1 - \omega_{*pe}/\omega + c^2 k_{\perp}^2 / \omega_{pe}^2} \right| \left| \frac{ck_{\parallel}}{\omega_{*e}} \right| \frac{1}{k_x r_n} \\ &\simeq \frac{ck_{\parallel}^0}{\omega_{*e}} \frac{1 + \eta_e}{k_x r_n [(\eta_e / 2\epsilon_n)^{1/2} + c^2 k_{\perp}^2 / \omega_{pe}^2]}, \end{aligned} \quad (71)$$

which is consistent with $k_{\parallel}^{nl} \simeq k_{\parallel}^0$.

Thus we argue that in the strongly unstable regime the fields saturate to within numerical constants at the level where $\Omega_E = \gamma_k$ and $k_{\parallel}^{nl} \simeq k_{\parallel}^0$, with $\bar{p}_e \simeq p_e' / |k_x|$. In this regime the actual electron motion is a stochastic diffusion since the conditions found in Refs. 11, 12, and 17 are satisfied.

B. Nonlinear model equations

To test the scaling arguments given in Sec. IV A and to determine the fluctuation spectrum quantitatively, we propose further theory and simulations of the dimensionless nonlinear equations derived in this section.

We define the dimensionless space-time variables by

$$x \rightarrow \rho_{ei} x, \quad y \rightarrow \rho_{ei} y, \quad z \rightarrow r_n z, \quad t \rightarrow r_n t / v_{ei}. \quad (72)$$

We scale the amplitude of the fields as follows:

$$\begin{aligned} \frac{\bar{p}_e}{p_e} &= \frac{\rho_{ei}}{r_n} \tilde{p}, \quad \frac{v_{\parallel e}}{v_{ei}} = \frac{\rho_{ei}}{r_n} v, \\ \frac{e\Phi}{T_e} &= \frac{\rho_{ei}}{r_n} \phi, \quad \frac{ev_{ei} A_{\parallel}}{c T_i} = \frac{\beta_i}{2} \frac{\rho_{ei}}{r_n} A, \end{aligned} \quad (73)$$

where $\beta_i = 8\pi n_i T_i / B^2$. The equations are simplified by considering the high density limit $\omega_{pe} \gg \omega_{ce}$ and using quasineutrality, where

$$\frac{\tilde{n}_e}{n_e} = \frac{\tilde{n}_i}{n_i} = - \frac{\tau \rho_{ei}}{r_n} \phi. \quad (74)$$

With these scalings Ampère's law reduces to

$$v = \nabla^2 A. \quad (75)$$

Using (74) and (75) to eliminate \tilde{n}_e and $v_{\parallel e}$ in Eqs. (54)–(56), we obtain the following three coupled field equations:

$$\begin{aligned} (1 - \nabla_{\perp}^2) \frac{\partial \phi}{\partial t} &= [1 - 2\epsilon_n + \tau(1 + \eta_e) \nabla_{\perp}^2] \frac{\partial \phi}{\partial y} \\ &\quad + 2\epsilon_n \frac{\partial \tilde{p}}{\partial y} + \tau[\phi, \nabla_{\perp}^2 \phi] \\ &\quad + \frac{1}{\tau} \left(\frac{\partial}{\partial z} \nabla_{\perp}^2 A - \frac{\beta_i}{2\tau} [A, \nabla_{\perp}^2 A] \right) + d_c \nabla_{\perp}^2 \phi, \end{aligned} \quad (76)$$

$$\begin{aligned} \left(\nabla_{\perp}^2 - \frac{\beta_i}{2} \right) \frac{\partial A}{\partial t} &= \tau \frac{\partial \phi}{\partial z} - \tau \frac{\beta_i}{2} [A, \phi] - \tau \frac{\partial \tilde{p}}{\partial z} + \frac{\beta_i}{2} [A, \tilde{p}] \\ &\quad + \tau \frac{(1 + \eta_e)}{2} \beta_i \frac{\partial A}{\partial y} - \tau[\phi, \nabla_{\perp}^2 A] \\ &\quad - \eta \nabla_{\perp}^2 A, \end{aligned} \quad (77)$$

$$\begin{aligned} \frac{\partial \tilde{p}}{\partial t} &= -[\tau(1 + \eta_e) - 2\Gamma\tau\epsilon_n] \frac{\partial \phi}{\partial y} - 2\Gamma\tau\epsilon_n \frac{\partial \tilde{p}}{\partial y} \\ &\quad - \tau[\phi, \tilde{p}] - 2\Gamma\tau\epsilon_n \frac{\partial}{\partial y} (\tilde{p} + \tau\phi) \\ &\quad - \Gamma \left(\frac{\partial \nabla_{\perp}^2 A}{\partial z} - \frac{\beta_i}{2\tau} [A, \nabla_{\perp}^2 A] \right) \\ &\quad + \kappa_{\perp} \nabla_{\perp}^2 \tilde{p} + \kappa_{\parallel} \nabla_{\parallel}^2 \tilde{p}. \end{aligned} \quad (78)$$

In Eqs. (76)–(78) we include electron cross-field diffusion, resistivity, and electron thermal conductivity to absorb energy transformed to $|k| \rightarrow \infty$, which is outside the range of validity of the fluid equations. Using the classical transport coefficients, the dimensionless coefficients are

$$d_c = \left(\frac{v_{ei} r_n}{v_{ei}} \right) \left(\frac{T_e}{T_i} \right), \quad \eta = 0.51 \left(\frac{v_{ei} r_n}{v_{ei}} \right),$$

$$\kappa_1 = 3.11 (v_{ei} r_n / v_{ei}) (T_e / T_i),$$

and

$$\kappa_{||} = 2.11 (v_{ei} / v_{ei} r_n) (T_e / T_i).$$

In reducing Eqs. (54)–(57) to (76)–(78) we assumed that the dominant nonlinearities are the $\mathbf{E} \times \mathbf{B}$ convective derivative and the $\mathbf{B} \cdot \nabla$ bending of the magnetic field lines resulting from the perturbations in the magnetic field lines. In writing these two nonlinearities it is convenient to introduce the Poisson bracket operator defined as follows:

$$\mathbf{B} \cdot \nabla f = -\hat{\mathbf{z}} \cdot \nabla A \times \nabla f \equiv -[A, f], \quad (79)$$

$$\mathbf{v}_E \cdot \nabla g = \hat{\mathbf{z}} \cdot \nabla \phi \times \nabla g \equiv [\phi, g], \quad (80)$$

with the property $[f, g]_y = -\partial_x [(\partial f / \partial y)(g)] = \partial_x [f(\partial g / \partial y)]$. We define the volume average by

$$\langle F \rangle = V^{-1} \int d^3x F(x, y, z, t) = L_x^{-1} \int dx \bar{F}(x, t)$$

and note the properties $\langle h[f, g] \rangle = \langle f[g, h] \rangle = \langle g[h, f] \rangle$.

The nonlinear model in Eqs. (76)–(78) reduces further for the case of flat density gradients $\eta_e \rightarrow \infty$. The reduction is given in the Appendix.

C. Anomalous fluxes and energy conservation

The essential cross-field correlation functions, such as $q_{es}(x) = \overline{(v_x \tilde{P}_e)}$, determine both the quasilinear evolution of $\tilde{P}_e(x, t)$ and the flow of fluctuation energy between the three field components of the total fluctuation energy $E = E_1 + E_2 + E_3$, where

$$\begin{aligned} E_1 &= E_\phi = \frac{1}{2} \langle \phi^2 + (\nabla \phi)^2 \rangle, \\ E_2 &= E_A = \frac{1}{2} \langle (\nabla^2 A)^2 + \beta_i / 2\tau (\nabla A)^2 \rangle, \\ E_3 &= E_p = \frac{1}{2} \langle (\tilde{P})^2 \rangle. \end{aligned} \quad (81)$$

The four cross-field correlation functions required for $\partial_t E_\alpha$ and $\partial_t \tilde{P}_e(x, t)$ are

$$\begin{aligned} q_{es}(x) &= \overline{(v_x \tilde{P}_e)} = - \left(\frac{\partial \phi}{\partial y} \tilde{P}_e \right), \\ q_{em}(x) &= \overline{\tilde{P}_e \left(\frac{B_x}{B} v \right)} = \overline{\tilde{P}_e \left(\frac{\partial A}{\partial y} v \right)}, \\ \dot{Q}(x) &= \overline{(v E_{||}^{es})} = - \overline{(v \hat{\mathbf{b}}_0 \cdot \nabla \phi)}, \\ \dot{W}(x) &= \overline{(\tilde{P}_e \hat{\mathbf{b}}_0 \cdot \nabla v)} = \left(\tilde{P} \frac{\partial v}{\partial z} \right), \end{aligned} \quad (82)$$

where $\hat{\mathbf{b}}_0 = \mathbf{B}_0 / |B| = \hat{\phi} + (\epsilon_n / q) \hat{\theta} \equiv \hat{\mathbf{z}}$. In Eqs. (82), q_{es} is the $\mathbf{E} \times \mathbf{B}$ flow of electron thermal heat and q_{em} is a magnetic flutter thermal flow. The work done by the parallel electric field on the electron fluid is \dot{Q} and the work done by the parallel compression of the electron pressure is \dot{W} . The fluctuation modified collisional transport flux is

$$q_{cl}(x) = -\kappa_1^e \frac{\partial \tilde{P}_e}{\partial x} + \kappa_{||}^e \frac{\beta_i}{2} \left(\frac{\partial A}{\partial y} \nabla_{||} \tilde{P} \right).$$

The net thermal balance equation follows from averaging over y, z and yields the transport equation

$$\begin{aligned} \frac{\partial \tilde{P}_e}{\partial t} &= - \frac{\partial}{\partial x} \left(\tilde{P}_e v_x + \tilde{P}_e \frac{v_{||e} B_x}{B} \right) - \frac{2}{3} \overline{\tilde{P}_e \nabla \cdot \mathbf{v}_E} \\ &\quad - \frac{2}{3} \overline{\tilde{P}_e \hat{\mathbf{b}}_0 \cdot \nabla v_{||e}} - \frac{2}{3} \tilde{P}_e \frac{\partial}{\partial x} \frac{v_{||e} B_x}{B} \\ &= -\partial_x (q_{es} + q_{cl}) - \frac{4}{3} q_{es} - \frac{2}{3} \dot{W} \\ &\quad - \frac{2}{3} \tilde{P}_e \frac{\partial}{\partial x} \left(\frac{q_{em}}{\tilde{P}_e} \right) + \frac{2}{3} P_e^{\text{ext}}, \end{aligned} \quad (83)$$

where P_e^{ext} is the externally injected electron heating. Subtracting $\partial \tilde{P}_e / \partial t$ from the total pressure balance leads to Eq. (78) for $\partial_t \tilde{P}_e$.

The energy balance equation can be written in several forms (Refs. 5–7). In terms of $E_{1,2,3}$ in Eq. (81) we have from Eqs. (76)–(78) that

$$\begin{aligned} \frac{dE_\phi}{dt} &= 2\epsilon_n \langle q_{es} \rangle + \frac{1}{\tau} \langle \dot{Q} \rangle - d_c \langle (\nabla_{\perp} \phi)^2 \rangle, \\ \frac{dE_A}{dt} &= -\tau \langle \dot{Q} \rangle + \tau \langle \dot{W} \rangle - \eta \langle (\nabla_{\perp} A)^2 \rangle, \\ \frac{dE_p}{dt} &= (1 + \eta_e) \langle q_{es} \rangle - 2\Gamma \tau \epsilon_n \langle q_{es} \rangle + 2\Gamma \tau^2 \epsilon_n \langle q_{es} \rangle \\ &\quad - \Gamma \langle \dot{W} \rangle - \kappa_{\perp} \langle (\nabla_{\perp} \tilde{P})^2 \rangle - \kappa_{||} \langle (\nabla_{||} \tilde{P})^2 \rangle. \end{aligned} \quad (84)$$

From which it follows that

$$E_T = E_\phi + (1/\tau^2) E_A + (1/\Gamma \tau) E_p \quad (85)$$

satisfies

$$\begin{aligned} \frac{dE_T}{dt} &= (1 + \eta_e) \langle q_{es} \rangle + 2\tau \epsilon_n \langle q_{es} \rangle \\ &\quad - d_c \langle (\nabla_{\perp} \phi)^2 \rangle - \eta \langle (\nabla_{\perp} A)^2 \rangle \\ &\quad - \kappa_{\perp} \langle (\nabla_{\perp} \tilde{P})^2 \rangle - \kappa_{||} \langle (\nabla_{||} \tilde{P})^2 \rangle. \end{aligned} \quad (86)$$

Further studies of the saturated nonlinear states predicted by Eqs. (76)–(78) are in progress to determine the dominant space scales and relative importance of the electromagnetic and electrostatic transport mechanisms.

D. Electron orbits and stochastic diffusion

Although the anomalous fluxes given in Eqs. (82) are straightforward to evaluate in the quasilinear approximation by using the linear fluctuations given in Eqs. (15), (16), and (50), the quasilinear approximation breaks down at the mixing length level of saturation (69). At the mixing length level the circulation time $1/\Omega_E$ around the electric vortex is comparable to the linear mode frequency. Renormalized electron-wave propagators $g_k^e(\mathbf{v}) = \langle (\omega - \omega_{De} - k_{||} v - \Omega_E + i\nu)^{-1} \rangle$ describe this regime for $R_E = \Omega_E \tau_c \lesssim 1$. The development of the anomalous flux formulas in the regime $R_E \lesssim 1$ is a complex procedure which is perhaps less useful than the alternate approach advanced by Horton *et al.*^{11,17}

For the toroidal transport problem the cross-field (x, y) electron motion is given by Eqs. (10) and (11) of Ref. 11:

$$\begin{aligned}\frac{dx}{dt} &= -\frac{c}{B} \frac{\partial \Phi}{\partial y} + \frac{v_{\parallel}}{B} \frac{\partial A}{\partial y} + v_D \sin \theta, \\ \frac{dy}{dt} &= \frac{c}{B} \frac{\partial \Phi}{\partial x} - \frac{v_{\parallel}}{B} \frac{\partial}{\partial x} (A_s + A) + v_D \cos \theta,\end{aligned}\quad (87)$$

with $A_s(x) = (B_0/2R)sx^2$, $v_D = (cT_e/eBR)(\frac{1}{2}v_{\perp}^2 + v_{\parallel}^2)/v_e^2$, and $\theta(t) = z(t)/qR$. In this model the parallel motion (z, v_{\parallel}) along \mathbf{b}_0 is given by the elliptic functions for trapped and circulating electrons.

For a ballooning mode fluctuation with $k_x = k_y s \theta$ the characteristic frequency shift resulting from the x, y motion in the mode is

$$\mathbf{k} \cdot \mathbf{v}_1 = \Omega^{nl} + \omega_{De} (v_{\perp}^2, v_{\parallel}^2) (\cos \theta + s \theta \sin \theta), \quad (88)$$

with

$$\Omega^{nl} = \mathbf{k} \cdot \tilde{\mathbf{v}}_E + v_{\parallel} (\mathbf{k}_{\perp} \cdot \tilde{\mathbf{B}}_1 / B_0) \equiv \Omega_E + k_{\parallel}^{nl} v_{\parallel}.$$

For $R_E \gtrsim 1$ the stochastic diffusion from the resonance $\Omega_E \sim |\omega_k|$ gives the anomalous transport

$$\chi_{es} \sim \tilde{v}_E / \langle k_x \rangle \sim \frac{\bar{\lambda}_x}{r_{Te}} \left(\frac{cT_e}{eB} \right) \approx \frac{c}{\omega_{pe} r_{Te}} \left(\frac{cT_e}{eB} \right), \quad (89)$$

using $\tilde{v}_E \sim \rho_{ei} v_{ei} / r_{Te}$ and the correlation length $\bar{\lambda}_x \sim c / \omega_{pe}$. For the longer wavelength part of the spectrum, the motion is stochastic from the resonance overlap $\Omega_E \sim k_{\parallel}^0 v_e$ for circulating electrons and from $\Omega_E \sim \omega_{be} = \epsilon^{1/2} v_e / qR$ for trapped electrons. In this regime the stochastic diffusion is dominated by trapped electrons and the net thermal diffusivity given by

$$\chi_{em} = \epsilon^{1/2} c^2 \omega_{be} / \omega_{pe}^2 = rc^2 v_e / qR^2 \omega_{pe}^2, \quad (90)$$

for $\Omega_E \gtrsim \omega_{be}$, implying the confinement time $\tau_E = a^2 / 4\chi_{em} = qaR^2 \omega_{pe}^2 / 4c^2 v_e$. The condition on the turbulence level can be expressed in terms of r_{Te} by using $\Omega_E \sim k_x \tilde{v}_{Ex}$ and $\gamma \delta \tilde{p}_e = \tilde{v}_{Ex} p'_e = \tilde{v}_{Ex} k_x \delta p_e$ to write $\Omega_E \simeq \gamma_k > \epsilon^{1/2} v_e / qR$. Note that Ref. 11 finds that Eq. (90) is independent of r_{Te} when the turbulence level satisfies the condition $\Omega_E \gtrsim \omega_{be}$.

The test particle transport simulations in Ref. 11 show that once the fluctuation levels are sufficient to produce global stochasticity, the deviations of the diffusion coefficient from Eq. (90) are rather weakly dependent on the details of the fluctuation spectrum used in the test particle Hamiltonian. This hypothesis was tested by using a 5×5 isotropic \mathbf{k}_1 space with $\phi(k_{\perp}) = \phi_0 / k_{\perp}^m$, where $m = 1, 2, 3$, and computing the stochastic diffusion coefficient for variable ϕ_1 , s , v_D and $u = \omega_k / k_y$. Once the electrons are globally stochastic the diffusion is essentially determined by the correlation scale length $l_c = 1 / \Delta k_{\perp}$ and the decorrelation rate $\tau_c^{-1} \simeq \Omega_E \simeq \omega_{be}$. The diffusion does increase with increasing ϕ_1 , but less rapidly than linearly.

The formula given in Eq. (90) differs from the results of Eq. (6) of Ref. 3 and Eq. (32) of Ref. 4,

$$\chi_e = 0.13 c^2 s \eta_e (1 + \eta_e) / \omega_{pe}^2 qR.$$

This result was derived from a quasilinear formulation and the use of linear sheared eigenvalue mode characteristics. The factor $\eta_e (1 + \eta_e)$ was reported to come from fitting the numerically computed result for ω_k . The value of $k_{\perp} \gtrsim \omega_{pe} / c$ is found using the amplitude limit $c\phi_k / B \simeq 2\pi\omega_k / k_{\perp}^2$ and

carrying out the k_{\perp} summation in the quasilinear transport formula for the resonant electrons. As noted in Sec. I, our result for the electron diffusivity differs significantly from that in Refs. 3 and 4 in that Eq. (90) does not show the strong, explicit dependence on η_e . Experimental evidence from H-mode plasmas suggests that χ_e should not contain a strong η_e dependence. Specifically, η_e is large in the bulk region of the H-mode discharges, but confinement is observed to be improved.

V. CONCLUSIONS

Using toroidal ballooning mode theory we show that the electron temperature gradient η_e drives the lower hybrid drift mode unstable because of charge separation from the unfavorable grad B and curvature drifts. We analyze the nonlocal hydrodynamic regime keeping the electron fluid compressibility and the FLR heat flux to obtain the stability threshold and characteristic unstable fluctuations. We compare these results with local kinetic theory where the wave electron resonance $g_k^e = [\omega - \omega_{De} (v_{\perp}^2, v_{\parallel}^2) + i\nu]^{-1}$ is kept along with $J_0^2(k_{\perp} v_{\perp} / \omega_{ce})$ and the driving force $\eta_e (v^2/2 - \frac{3}{2})$ to obtain the kinetic theory threshold and spectrum of linearly unstable fluctuations.

Including magnetic perturbations from A_{\parallel} in the hydrodynamic analysis we show that the short wavelength regime $k_{\perp} \simeq \omega_{ce} / v_e$ is electrostatic with substantial growth rate $\gamma_k \sim |\omega_k| \gtrsim k_{\parallel} v_e$, while the long wavelength regime $k_{\perp} \sim \omega_{pe} / c$ is neutrally stable with $E_{\parallel} \ll |k_{\parallel} \Phi|$.

We introduce a nonlinear hydrodynamic model with the fields ϕ , A , and δp_e that is closely related to earlier η_i -mode models⁵⁻⁷ and the electromagnetic edge turbulence equations of Bekki and Kaneda.¹⁸ For the nonlinear model we find only the energy integral of the motion for the isolated, dissipationless system. For the unstable, dissipative system we may thus expect a result between the two-dimensional (2-D) inverse cascade and the 3-D cascade, since the system is only weakly 3-D with $\nabla_{\perp} \gg \nabla_{\parallel}$. We suggest that it is important to perform a complete analysis of this nonlinear model system for the amplitude and fluctuation spectrum of this drift wavelike system. Here we give the mixing length formulas for the expected saturation level with $k_{\parallel}^{nl} \simeq k_{\parallel}^0$ and $\Omega_E \sim \omega_k \sim \gamma_k$.

We note here that similar equations without magnetic shear are solved by Bekki and Kaneda¹⁸ for electromagnetic edge turbulence. In that work with a $32 \times 32 \times 16$ grid the buildup of large amplitude low k_{\perp} modes is reported. That simulation shows that the transport is dominated by $k_z = 0$. In the present problem we expect nonlinear magnetic vortices with $k_{\parallel}^{nl} + k_{\parallel}^0 \simeq 0$ may arise for not too strong a magnetic shear $s < 2q$.

For saturated mode spectra of the form ϕ_1 / k_{\perp}^m , with $m = 1, 2, 3$, the associated vortex circulation frequencies are of the form $\Omega_E \sim \phi_1 k_{\perp}^p$, with $p = -1, 0, +1$, with the evolution of distributions of test electrons given in tokamak geometry by Horton *et al.*¹¹ For the long wavelength $k_{\perp} \sim \omega_{pe} / c$ part of the spectrum, the stochasticity arises from the overlapping of the z, v_{\parallel} resonance with the Ω_E , ω_{De} , and $k_{\parallel}^{nl} v_{\parallel}$ motions producing a strong diffusion of the trapped elec-

trons and a weak diffusion of the passing electrons. In this regime we predict the neo-Alcator or Merezhkin-Mukhovatov formula (90) for the thermal diffusivity.^{1,2}

In summary, the present work shows that the toroidal electron temperature gradient driven lower hybrid turbulence leads to an injection of small scale ρ_{ei} turbulence at or just above the transit electron frequency, as shown in Fig. 6. The small scale electrostatic turbulence directly produces the anomalous χ_e given in Eqs. (46) and (47), which is larger than the electron neoclassical plateau value, but small compared with the electron diffusivity obtained from c/ω_{pe} and ρ_s scale drift turbulence. The importance of the ρ_{ei} turbulence, however, is the injection of a drift wave turbulence near the electron transit and bounce frequencies, together with the known property of the quasi-2-D ($\nabla_\perp \gg \nabla_\parallel$) drift turbulence to mode couple energy to both larger and smaller spatial scales.

The theory presented has direct implications for the χ_e formulas given by Horton *et al.*¹¹ and Parail and Yushmanov.¹² In Ref. 11 the transition from c/ω_{pe} to ρ_s -scale turbulent transport was reported from test electron diffusion theory and simulations. Recent transport studies by Parail and Yushmanov¹⁹ based on the transitional formulas derived in Ref. 11 for c/ω_{pe} and ρ_s -scale drift turbulence explain well the power balance χ_e in both Ohmic and auxiliary heated tokamak discharges. The present work presents a mechanism in toroidal geometry that may explain the source of this turbulence and the associated anomalous electron transport. In particular, we suggest here a subregime in the transition from the low density neo-Alcator and Merezhkin-Mukhovatov scaling given in Eq. (90) to a modified c/ω_{pe} scaling given by Eq. (89) at higher density or beta poloidal. At still higher values of beta poloidal, the transport is given by the ρ_s -scale turbulence in Ref. 11 and compared with

experimental power balance studies by Parail and Yushmanov.¹⁹

From the theoretical point of view, further work using nonlinear simulations and transport theory will be required to determine the conditions for the transitions between the regimes and to estimate the numerical coefficients in the transport formulas. Nevertheless, from an experimental point of view the existence of such electron instabilities which appear as the direct analog of the toroidal η_i -mode turbulence⁶ may be sufficient reason for adopting the associated anomalous χ_e formulas for empirical studies of power balance in tokamaks.

ACKNOWLEDGMENTS

The authors gratefully acknowledge useful conversations with D.-I. Choi, P. N. Guzdar, T. Tajima, and Y.-Z. Zhang during the course of this work.

This work was supported in part by the Korea Science and Engineering Foundation (B. G. Hong) and the U.S. Department of Energy.

APPENDIX: REDUCED NONLINEAR MODEL EQUATIONS IN H-MODE PLASMA

For flat density profiles, it is important to redefine the dimensionless space-time variables by

$$x \rightarrow \rho_{ei} x, \quad y \rightarrow \rho_{ei} y, \quad z \rightarrow r_T z, \quad t \rightarrow r_T t / v_{ei}. \quad (A1)$$

We rescale the amplitude of the fields as follows:

$$\begin{aligned} \frac{\tilde{P}_e}{P_e} &= \frac{\rho_{ei}}{r_T} P, & \frac{v_{||e}}{v_{ei}} &= \frac{\rho_{ei}}{r_T} v, \\ \frac{e\Phi}{T_e} &= \frac{\rho_{ei}}{r_T} \phi, & \frac{ev_{ei} A_{||}}{cT_e} &= \frac{\beta_i}{2} \frac{\rho_{ei}}{r_T} A. \end{aligned} \quad (A2)$$

Then, Eqs. (76) and (77) reduce to

$$\begin{aligned} (1 - \nabla_\perp^2) \frac{\partial \phi}{\partial t} &= \left(\eta_e^{-1} - 2 \frac{r_T}{R} + \tau (\eta_e^{-1} + 1) \nabla_\perp^2 \right) \frac{\partial \phi}{\partial y} \\ &+ 2 \frac{r_T}{R} \frac{\partial}{\partial y} P + \tau [\phi, \nabla_\perp^2 \phi] \\ &+ \frac{1}{\tau} \left(\frac{\partial}{\partial z} \nabla_\perp^2 A - \frac{\beta_i}{2\tau} [A, \nabla_\perp^2 A] \right) + d_c' \nabla_\perp^2 \phi, \end{aligned} \quad (A3)$$

$$\begin{aligned} \left(\nabla_\perp^2 - \frac{\beta_i}{2} \right) \frac{\partial A}{\partial t} &= \frac{\partial \phi}{\partial z} - \tau \frac{\beta_i}{2} [A, \phi] - \tau \frac{\partial P}{\partial z} + \frac{\beta_i}{2} [A, P_e] \\ &+ \tau (\eta_e^{-1} + 1) \frac{\beta_i}{2} \frac{\partial A}{\partial y} - \tau [\phi, \nabla_\perp^2 A] \\ &- \eta' \nabla_\perp^2 A, \end{aligned} \quad (A4)$$

$$\begin{aligned} \frac{\partial P}{\partial t} &= - \left(\tau (\eta_e^{-1} + 1) - \frac{2\Gamma\tau r_T}{R} \right) \frac{\partial \phi}{\partial y} - 2\Gamma\tau \frac{r_T}{R} \frac{\partial P}{\partial y} \\ &- \tau [\phi, P] - 2\Gamma\tau \frac{r_T}{R} \frac{\partial}{\partial y} (P + \tau \phi) \end{aligned}$$

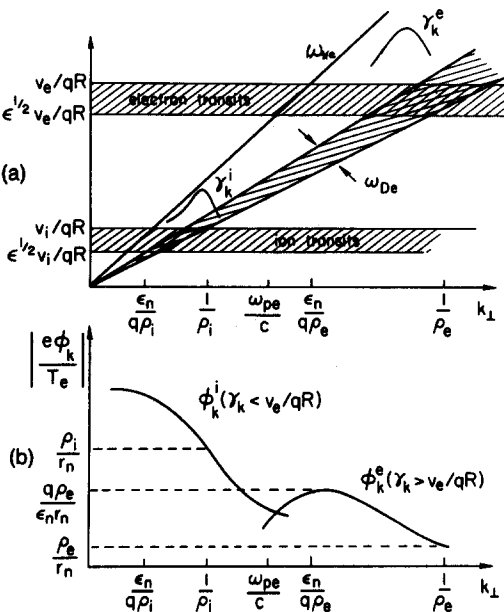


FIG. 6. Qualitative diagram of the k_\perp - ω fluctuation spectrum. (a) Characteristic frequencies and resonances versus inverse scale length k_\perp and (b) the associated mixing length level of the fluctuation or vortex amplitude as a function scale size.

$$- \Gamma \left(\frac{\partial}{\partial z} \nabla_{\perp}^2 A - \frac{\beta_i}{2} [A, \nabla_{\perp}^2 A] \right) - \frac{\beta_i}{2} [A, \nabla_{\perp}^2 A] - \kappa'_{\perp} \nabla_{\perp}^2 P - \kappa'_{\parallel} \nabla_{\parallel}^2 P. \quad (\text{A8})$$

$$- \kappa'_{\perp} \nabla_{\perp}^2 P - \kappa'_{\parallel} \nabla_{\parallel}^2 P, \quad (\text{A5})$$

where $d'_c = \eta_e^{-1} d_c$, $\eta'_{\parallel} = \eta_e^{-1} \eta$, $\kappa'_{\perp} = \eta_e^{-1} \kappa_{\perp}$, and $\kappa'_{\parallel} = \eta_e^{-1} \kappa_{\parallel}$. For $r_n > R/2$, Eqs. (A3)–(A5) reduce to

$$(1 - \nabla_{\perp}^2) \frac{\partial \phi}{\partial t} = (-2\epsilon_T + \tau \nabla_{\perp}^2) \frac{\partial \phi}{\partial y} + 2\epsilon_T \frac{\partial}{\partial y} P + \tau [\phi, \nabla_{\perp}^2 \phi] + \frac{1}{\tau} \left(\frac{\partial}{\partial z} \nabla_{\perp}^2 A - \frac{\beta_i}{2\tau} [A, \nabla_{\perp}^2 A] \right) + d'_c \nabla_{\perp}^2 \phi, \quad (\text{A6})$$

$$\left(\nabla_{\perp}^2 - \frac{\beta_i}{2} \right) \frac{\partial A}{\partial t} = \frac{\partial \phi}{\partial z} - \tau \frac{\beta_i}{2} [A, \phi] - \tau \frac{\partial P}{\partial z} + \tau \frac{\beta_i}{2} [A, P] + \tau \frac{\beta_i}{2} \frac{\partial A}{\partial y} - \tau [\phi, \nabla_{\perp}^2 A] - \eta' \nabla_{\perp}^2 A, \quad (\text{A7})$$

$$\left(\frac{\partial P}{\partial t} \right) = (-\tau + 2\Gamma\epsilon_T) \frac{\partial \phi}{\partial y} - 2\Gamma\epsilon_T \frac{\partial P}{\partial y} - \tau [\phi, P] - 2\Gamma\epsilon_T \frac{\partial}{\partial y} (P + \tau \phi) - \Gamma \left(\frac{\partial}{\partial z} \nabla_{\perp}^2 A \right)$$

¹R. R. Parker, M. Greenwald, S. C. Luckhardt, E. S. Marmor, M. Porkolab, and S. M. Wolf, Nucl. Fusion **25**, 1127 (1985).

²R. J. Goldston, Plasma Phys. Controlled Fusion **26**, 87 (1984).

³P. N. Guzdar, C. S. Liu, J. Q. Dong, and Y. C. Lee, Phys. Rev. Lett. **57**, 2818 (1986).

⁴Y. C. Lee, J. Q. Dong, P. N. Guzdar, and C. S. Liu, Phys. Fluids **30**, 1331 (1987).

⁵W. Horton, R. D. Estes, and D. Biskamp, Plasma Phys. **22**, 663 (1980).

⁶W. Horton, D.-I. Choi, and W. M. Tang, Phys. Fluids **24**, 1077 (1981).

⁷D. Brock and W. Horton, Plasma Phys. **24**, 271 (1982).

⁸B. G. Hong, D.-I. Choi, and W. Horton, Phys. Fluids **29**, 1872 (1986).

⁹W. Horton, J. E. Sedlak, D.-I. Choi, and B.-G. Hong, Phys. Fluids **28**, 3050 (1985).

¹⁰A. Jarmén, P. Andersson, and J. Weiland, Nucl. Fusion **27**, 941 (1987).

¹¹W. Horton, D.-I. Choi, P. N. Yushmanov, and V. V. Parail, Plasma Phys. Controlled Fusion **29**, 901 (1987).

¹²V. V. Parail and P. N. Yushmanov, JETP Lett. **42**, 278 (1985).

¹³R. R. Dominguez and R. W. Moore, Nucl. Fusion **26**, 85 (1986).

¹⁴F. Wagner, G. Becker, K. Behringer, D. Campbell, A. Eberhagen, W. Engelhardt, G. Fussmann, O. Gehre, J. Gernhardt, G. V. Gierke, G. Hass, M. Huang, F. Karger, M. Keilhacker, O. Klüber, M. Kornherr, K. Lackner, G. Lisitano, G. G. Lister, H. M. Mayer, D. Meisel, E. R. Müller, H. Murmann, N. Niedermeyer, W. Poschenrieder, H. Rapp, H. Röhr, F. Schneider, G. Siller, E. Speth, A. Stäbler, K. H. Steuer, G. Venus, O. Vollmer, and Z. Yu, Phys. Rev. Lett. **49**, 1408 (1982).

¹⁵W. M. Tang, G. Rewoldt, and L. Chen, Phys. Fluids **29**, 3715 (1986).

¹⁶R. R. Dominguez and R. E. Waltz, Phys. Fluids **31**, 3147 (1988).

¹⁷W. Horton, Plasma Phys. Controlled Fusion **27**, 937 (1985).

¹⁸N. Bekki and Y. Kaneda, Phys. Rev. Lett. **57**, 2176 (1986).

¹⁹V. V. Parail and P. N. Yushmanov (private communication, 1987).